

See discussions, stats, and author profiles for this publication at: <https://www.researchgate.net/publication/234055231>

# Chemical Kinetics of Biomass Pyrolysis

ARTICLE *in* ENERGY & FUELS · JANUARY 2009

Impact Factor: 2.79 · DOI: 10.1021/ef800551t

CITATIONS

168

READS

503

7 AUTHORS, INCLUDING:



[Eliseo Ranzi](#)

Politecnico di Milano

225 PUBLICATIONS 4,783 CITATIONS

[SEE PROFILE](#)



[Alberto Cuoci](#)

Politecnico di Milano

91 PUBLICATIONS 1,001 CITATIONS

[SEE PROFILE](#)



[Alessio Frassoldati](#)

Politecnico di Milano

106 PUBLICATIONS 1,845 CITATIONS

[SEE PROFILE](#)



[Sauro Pierucci](#)

Politecnico di Milano

61 PUBLICATIONS 839 CITATIONS

[SEE PROFILE](#)

## Chemical Kinetics of Biomass Pyrolysis

Eliseo Ranzi, Alberto Cuoci, Tiziano Faravelli, Alessio Frassoldati,  
Gabriele Migliavacca, Sauro Pierucci, and Samuele Sommariva

*Energy Fuels*, **2008**, 22 (6), 4292-4300 • DOI: 10.1021/ef800551t • Publication Date (Web): 14 October 2008

Downloaded from <http://pubs.acs.org> on February 26, 2009

### More About This Article

Additional resources and features associated with this article are available within the HTML version:

- Supporting Information
- Access to high resolution figures
- Links to articles and content related to this article
- Copyright permission to reproduce figures and/or text from this article

[View the Full Text HTML](#)



**ACS Publications**  
High quality. High impact.

Energy & Fuels is published by the American Chemical Society, 1155 Sixteenth Street N.W., Washington, DC 20036

# Chemical Kinetics of Biomass Pyrolysis

Eliseo Ranzi,<sup>\*,†</sup> Alberto Cuoci,<sup>†</sup> Tiziano Faravelli,<sup>†</sup> Alessio Frassoldati,<sup>†</sup>  
Gabriele Migliavacca,<sup>‡</sup> Sauro Pierucci,<sup>†</sup> and Samuele Sommariva<sup>†</sup>

CMIC, Department Politecnico di Milano, Piazza L. Da Vinci 32, 20133 Milano, Italy, and SSC,  
Stazione Sperimentale per i Combustibili, San Donato Milanese, Milano, Italy

Received July 11, 2008

This paper analyzes the main kinetic features of biomass pyrolysis, devolatilization, and the gas phase reactions of the released species. Three complex steps are faced in sequence: the characterization of biomasses, the description of the release of the species, and finally, their chemical evolution in the gas phase. Biomass is characterized as a mixture of reference constituents: cellulose, hemicellulose, and lignin. This assumption is verified versus experimental data, mainly relating to thermal degradation of different biomasses. Devolatilization of biomasses is a complex process in which several chemical reactions take place in both the gas and the condensed phase alongside the mass and thermal resistances involved in the pyrolysis process. A novel characterization of the released species is applied in the proposed devolatilization models. The successive gas phase reactions of released species are included into an existing detailed kinetic scheme of pyrolysis and oxidation of hydrocarbon fuels. Comparisons with experimental measurements in a drop tube reactor confirm the high potentials of the proposed modeling approach.

## 1. Introduction

Biomasses, because of the negligible impact on greenhouse effect, are an interesting answer to the growing demand of renewable energy. Researches have carried out characterizations of biomass pyrolysis, gasification, and combustion in order to design efficient and environmentally sustainable units. Biomass properties can significantly influence both heat transfer and reaction rates such that the optimal operating conditions are highly variable. Therefore, times, yields, and emissions depend on the original biomass source. The key to understanding the complex phenomena occurring inside the process units thus lies in the characterization of the initial biomasses and in describing the primary devolatilization phase, the released products, the gasification phase, and the secondary or successive gas phase reactions.

In a recent paper, Di Blasi<sup>1</sup> observed that large-scale development of devolatilization units requires significant efforts in the mathematical modeling that is to create powerful tools for designing and simulating reactor performances, understanding pollutants evolution, analyzing process transients, and examining strategies for effective control. Thermo-chemical conversion of biomasses in practical systems results from a strong interaction between chemical and physical processes at the levels of both the single particle and the surrounding environment. Therefore, models need an appropriate description in relation both to chemical kinetics and to transport phenomena.

The operating conditions and the biomass pyrolysis units can maximize the yields of tars and condensable products or char.<sup>2–4</sup> In the former case, the conversion process is indicated as fast

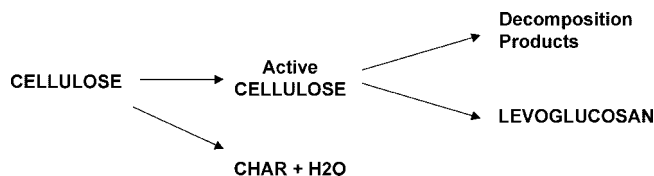


Figure 1. Multistep lumped mechanism of cellulose pyrolysis.

pyrolysis<sup>5</sup> and, after cooling and condensation, bio-oil is obtained. Fast pyrolysis requires high heating and heat transfer rates in the reaction zone, a primary conversion temperature of about 800 K, and short residence time of products in the vapor phase (below 2 s at about 700 K) with a rapid cooling of the vapor-phase products to limit the extent of secondary reactions. Conversely, the conventional, or slow pyrolysis, process produces comparable yields of char, gas, and tar species. It is important to describe the evolution of gas and tar volatile products as a function of the process conditions. Yields of CO and H<sub>2</sub> are the desired products of the gasification process and are favored by these secondary pyrolysis reactions of volatile species. Thermodynamic and equilibrium models are not accurate enough to design biomass gasifiers. They overestimate the yields of H<sub>2</sub> and CO, underestimate CO<sub>2</sub> yield, and predict a gas that is virtually free of CH<sub>4</sub> and heavier species.<sup>6</sup>

A mechanistic model of biomass pyrolysis was developed at the particle scale in order to describe the relative role of reaction kinetics and transport resistances.<sup>7</sup> Because of its mechanistic

\* To whom correspondence should be addressed. Phone: +39 02 23993250; fax: +39 02 70638173; e-mail: eliseo.ranzi@polimi.it.

<sup>†</sup> CMIC.

<sup>‡</sup> SSC.

(1) Di Blasi, C. Modeling chemical and physical processes of wood and biomass pyrolysis. *Prog. Energy Combust. Sci.* **2008**, *34*, 47–90.

(2) Bridgwater, A. V. Principles and practice of biomass fast pyrolysis processes for liquids. *J. Anal. Appl. Pyrol.* **1999**, *51*, 3–22.

(3) Bridgwater, A. V. Renewable fuels and chemicals by thermal processing of biomass. *Chem. Eng. J.* **2003**, *91*, 87–102.

(4) Antal, M. J.; Mochizuki, K.; Paredes, L. S. Flash carbonization of biomass. *Ind Eng. Chem. Res.* **2003**, *42*, 3690–9.

(5) Bridgwater, A. V.; Peacocke, G. V. C. Fast pyrolysis processes for biomass. *Renewable Sustainable Energy Rev.* **2000**, *4* (1), 1–73.

(6) Dupont, C.; Boissonnet, G.; Seiler, J. M.; Gauthier, P.; Schweich, D. *Fuel* **2007**, *86*, 32–40.

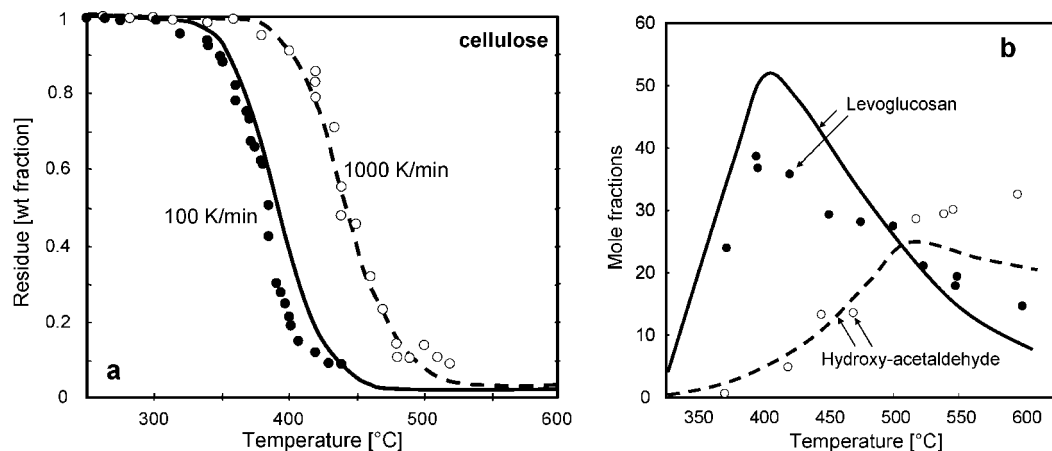


**Figure 2.** Pyrolysis of cellulose. Panel a: comparisons of model predictions (lines) and experimental data (points).<sup>30</sup> Panel b: Levoglucosan and hydroxyl-acetaldehyde. Comparisons of model predictions (lines) and experimental data (points).<sup>31</sup>

**Table 1. Lumped Kinetic Scheme of Cellulose Pyrolysis**

reaction	rate	units
CELL → CELLA	$k = 8 \times 10^{13} \exp(-46000/RT)$	$[s^{-1}]$
CELLA → 0.95 HAA + 0.25 Glyoxal + 0.20 CH <sub>3</sub> CHO + 0.20 C <sub>3</sub> H <sub>6</sub> O + 0.25 HMFU + 0.20 CO <sub>2</sub> + 0.15 CO + 0.1 CH <sub>4</sub> + 0.9 H <sub>2</sub> O + 0.65 Char	$k = 1 \times 10^9 \exp(-30000/RT)$	$[s^{-1}]$
CELLA → LVG	$k = 4T \exp(-10000/RT)$	$[s^{-1}]$
CELL → 5 H <sub>2</sub> O + 6 Char	$k = 8 \times 10^7 \exp(-32000/RT)$	$[s^{-1}]$

**Table 2. Lumped Kinetic Scheme of Hemicellulose Pyrolysis**

reaction	rate	units
HCE → 0.4 HCE1 + 0.6 HCE2	$k = 1 \times 10^{10} \exp(-31000/RT)$	$[s^{-1}]$
HCE1 → 2.5 H <sub>2</sub> + 0.125 H <sub>2</sub> O + CO + CO <sub>2</sub> + 0.5 CH <sub>2</sub> O + 0.25 CH <sub>3</sub> OH + 0.125 C <sub>2</sub> H <sub>5</sub> OH + 2 Char	$k = 3 \times 10^9 \exp(-27000/RT)$	$[s^{-1}]$
HCE1 → XYLOSE	$k = 3T \exp(-11000/RT)$	$[s^{-1}]$
HCE2 → 1.5 H <sub>2</sub> + 0.125 H <sub>2</sub> O + 0.2 CO <sub>2</sub> + 0.7 CH <sub>2</sub> O + 0.25 CH <sub>3</sub> OH + 0.125 C <sub>2</sub> H <sub>5</sub> OH + 0.8 G{CO <sub>2</sub> } + 0.8 G{COH <sub>2</sub> } + 2 Char	$k = 1 \times 10^{10} \exp(-33000/RT)$	$[s^{-1}]$

nature, it is not limited to a specific gasifier unit under a narrow range of conditions, but can be easily applied to different reactor types.

Beside heat and mass transport processes, a mechanistic kinetic model of biomass gasification and pyrolysis should focus on four different facets of the overall process:

- biomass characterization;
- biomass pyrolysis or devolatilization, that is, the decomposition of the solid into permanent gases, condensable vapors (tars) and solid residue (char);
- secondary gas phase reactions of the released gas and tar species;

(iv) char gasification and combustion, that is, the overall set of heterogeneous reactions of the gases (steam, O<sub>2</sub>, etc.) with the solid residue.

We will only discuss the first three features, characterization, pyrolysis, and gas phase reactions, whereas combustion of residual char is beyond the scope of this paper.

Biomasses are usually simply described in terms of the three major constituents: hemicellulose, cellulose, and lignin. Several recent works assume the noninteraction hypothesis in the thermal decomposition of these three constituents. Predictions from these models correctly reproduce the experimental thermogravimetric

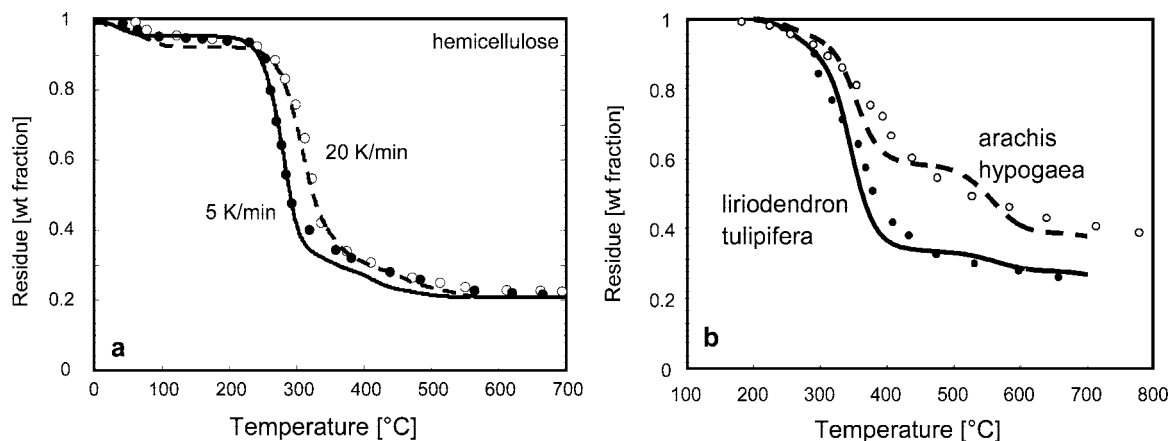


**Figure 3.** Panel a: pyrolysis of hemicellulose. Comparisons of model predictions (lines) and experimental data (points).<sup>32</sup> Panel b: pyrolysis of lignins (heating rates = 20 °C/min). Comparisons of model predictions (lines) and experimental data (points).<sup>34</sup>

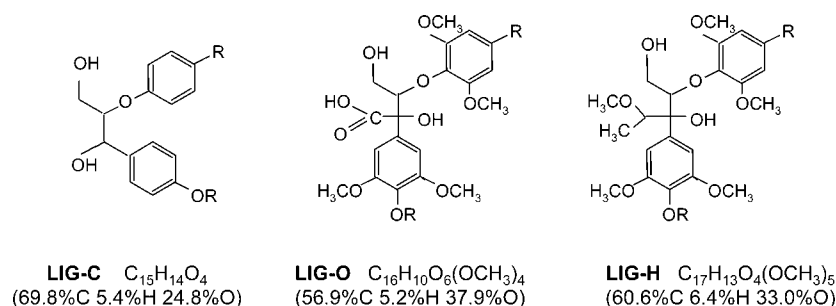
Scheme 1. Structures of **LIG-C**, **LIG-O**, and **LIG-H**

Table 3. Lumped Kinetic Scheme of Lignin Pyrolysis

reaction	rate	units
LIG-C $\rightarrow$ 0.35 LIG <sub>CC</sub> + 0.1 pCoumaryl + 0.08 Phenol + 1.49 H <sub>2</sub> + H <sub>2</sub> O + 1.32 G{COH <sub>2</sub> } + 7.05 Char	$k = 4 \times 10^{15} \exp(-48500/RT)$	[s <sup>-1</sup> ]
LIG-H $\rightarrow$ LIG <sub>OH</sub> + C <sub>3</sub> H <sub>6</sub> O	$k = 2 \times 10^{13} \exp(-37500/RT)$	[s <sup>-1</sup> ]
LIG-O $\rightarrow$ LIG <sub>OH</sub> + CO <sub>2</sub>	$k = 1. \times 10^9 \exp(-25500/RT)$	[s <sup>-1</sup> ]
LIG <sub>CC</sub> $\rightarrow$ 0.3 pCoumaryl + 0.2 Phenol + 0.35 C <sub>3</sub> H <sub>4</sub> O <sub>2</sub> + 1.2 H <sub>2</sub> + 0.7 H <sub>2</sub> O + 0.25 CH <sub>4</sub> + 0.25 C <sub>2</sub> H <sub>4</sub> + 1.3 G{COH <sub>2</sub> } + 0.5 G{CO} + 7.5 Char	$k = 5 \times 10^6 \exp(-31500/RT)$	[s <sup>-1</sup> ]
LIG <sub>OH</sub> $\rightarrow$ LIG + 0.5 H <sub>2</sub> + H <sub>2</sub> O + CH <sub>3</sub> OH + G{CO} + 1.5 G{COH <sub>2</sub> } + 5 Char	$k = 10^{13} \times \exp(-49500/RT)$	[s <sup>-1</sup> ]
LIG $\rightarrow$ C <sub>11</sub> H <sub>12</sub> O <sub>4</sub>	$k = 10^5 \times \exp(-20500/RT)$	[s <sup>-1</sup> ]
LIG $\rightarrow$ 0.7 H <sub>2</sub> + H <sub>2</sub> O + 0.2 CH <sub>2</sub> O + 0.5 CO + 0.2 CH <sub>2</sub> O + 0.4 CH <sub>3</sub> OH + 0.2 CH <sub>3</sub> CHO + 0.2 C <sub>3</sub> H <sub>6</sub> O <sub>2</sub> + 4 CH <sub>4</sub> + 0.5 C <sub>2</sub> H <sub>4</sub> + G{CO} + 0.5 G{COH <sub>2</sub> } + 6 Char	$k = 8 \times 10^1 \times T \times \exp(-12000/RT)$	[s <sup>-1</sup> ]
	$k = 1.2 \times 10^9 \exp(-30000/RT)$	[s <sup>-1</sup> ]

(TG) curves during the pyrolysis of several biomasses.<sup>8–10</sup> However Hosoya et al.<sup>11</sup> recently contradicted these assumption by demonstrating the existence of cellulose–hemicellulose and cellulose–lignin interactions in wood pyrolysis at gasification temperature.

Devolatilization is mainly investigated on the basis of the overall residue prediction, gas and tar formation, without significant efforts toward a chemical characterization of the released species, including stable end-product gases. These studies are mainly restricted to the kinetically controlled regime, so that the heating program and the particle sizes are chosen in order to minimize the effects of various transport processes. Accordingly, these results are not very useful for the design of industrial units.

Recent literature provides interesting examples of a more complete picture of biomass pyrolysis by taking into account the total devolatilization and gas evolution.<sup>12–14</sup> Fourier trans-

form infrared (FTIR) analysis and TG-mass spectrometry (TG-MS) techniques proved to have a good potential to perform accurate and valuable measures of volatile species, as recently discussed by Biagini et al.<sup>15</sup> and by Worasuwannarak et al.<sup>16</sup>

Modeling biomass pyrolysis is a challenge because of the variety of the raw materials involved and also because of the wide operating conditions. As already observed and discussed by Shin et al.,<sup>17</sup> the accurate predictions of gas species and aromatics from the pyrolysis of biomasses, and mainly the effect of different operating conditions, not only require the description of the released components, but also the definition of their successive gas phase reactions.

The central topics covered in this paper are, first, the characterization of biomasses and, then, the chemistry of devolatilization process. This work aims at giving a contribution to a better understanding of biomass pyrolysis not only with a novel characterization of the chemical nature of the released species, but also with a detailed description of the successive gas phase reactions.

The proposed model of biomass pyrolysis is based on conventional multistep devolatilization models of the three main biomass components (cellulose, hemicellulose, and lignin) and predicts the yields and lumped composition of gas, tar, and solid residue.

Secondary or successive gas phase reactions of the released volatile species are also described with considerable detail and are coupled to a more general kinetic scheme of pyrolysis and oxidation of hydrocarbon species.

The overall aim of this paper is to give a first evidence of the reliability and possibilities of chemical reaction engineering in the field of biomass gasification to produce syngas and/or

(7) Pierucci, S.; Ranzi, E. A general mathematical model for a moving bed gasifier, 18th European Symposium on Computer Aided Process Engineering, Lyon, France, June 1–4, 2008; *ESCAPE 18*; Braunschweig, B., Loulia, X. Eds; Elsevier B.V.: 2008.

(8) Manya, J. J.; Velo, E.; Puigjaner, L. Kinetics of Biomass Pyrolysis: a Reformulated Three-Parallel-Reactions Model. *Ind. Eng. Chem. Res.* **2003**, *42*, 434–44.

(9) Becidan, M.; Varhegyi, G.; Hustad, J. E. Skreiberg, Thermal Decomposition of Biomass Wastes. A Kinetic Study. *Ind. Eng. Chem. Res.* **2007**, *46*, 2428–2437.

(10) Miranda, R. C.; Sosa-Blanco, D.; Bustos-Martinez, C. Vase Pyrolysis of textile wastes Note I. Kinetics and yields. *J. Anal. Appl. Pyrolysis* **2007**, *80*, 489–495.

(11) Hosoya, T.; Kawamoto, H.; Saka, S. Cellulose-hemicellulose and cellulose-lignin interactions in wood pyrolysis at gasification temperature. *J. Anal. Appl. Pyrolysis* **2007**, *80* (1), 118–125.

(12) Radmanesh, R.; Courbariaux, Y.; Chaouki, J.; C.; Guy. A unified lumped approach in kinetic modeling of biomass pyrolysis. *Fuel* **2006**, *85*, 1211–1220.

(13) Yanik, J.; Kornmayer, C.; Saglam, M.; Yüksel, M. Fast pyrolysis of agricultural wastes: Characterization of pyrolysis products. *Fuel Processing Technology* ( **2007** ), *88* (10), 942–947.

(14) De Jong, W.; G.; Di Nola; Venneker, B. C. H.; Spliethoff, H.; Wojtowicz, A., M. TG-FTIR pyrolysis of coal and secondary biomass fuels: Determination of pyrolysis kinetic parameters for main species and NOx precursors. *Fuel* **2007**, *86*, 2367–2376.

(15) Biagini, E.; Barontini, F.; Tognotti, L. Devolatilization of Biomass Fuels and Biomass Components Studied by TG/FTIR Technique. *Ind. Eng. Chem. Res.* **2006**, *45*, 4486–4493.

(16) Worasuwannarak, N.; Sonobe, T.; Tanthapanichakoon, W. Pyrolysis behaviors of rice straw, rice husk, and corn cob by TG-MS technique. *J. Anal. Appl. Pyrolysis* **2007**, *78*, 265–271.

(17) Shin, E. J.; Nimlos, M. R.; Evans, R. J. *Fuel* **2001**, *80*, 1697–1709.

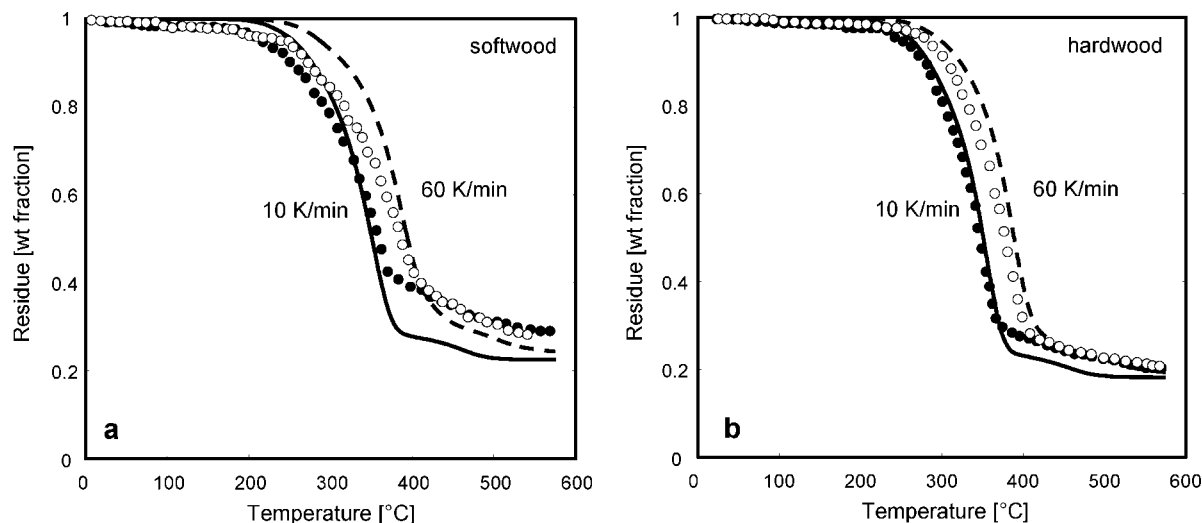


Figure 4. TG curves of softwood and hardwood biomasses at different heating rate (points: experimental data;<sup>35</sup> lines: model predictions).

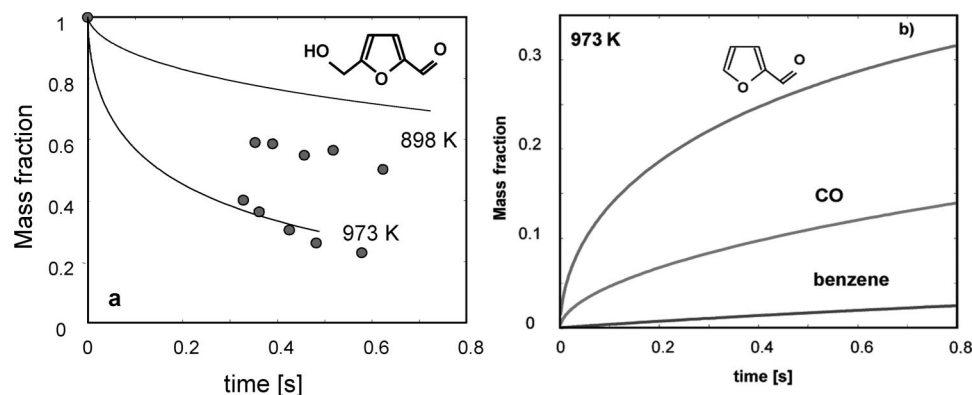


Figure 5. Pyrolysis of 5-hydroxymethyl-furfural. Panel a: Comparisons between model predictions (lines) and experimental measurements (points).<sup>17</sup> Panel b: relevant intermediate products.

bio-oils and chemicals. The proposed models, even though still quite simple, increase the complexity, with respect to one- or two-step degradation mechanisms, in order to take into account the main volatilization products and their successive fate in the gas phase.

## 2. Characterization of Biomasses and Pyrolysis of Reference Components

The biochemical analysis of biomasses provides information on cellulose, hemicellulose, and lignin content together with extractives and ash. Although extractives, either soluble in water or in organic solvents, usually account for less than 10% of the total biomass, they are ignored as participating to its characterization. Phenolic compounds, alkaloids, nonproteic amino acids, terpenes, and fatty acids are just a few examples of the species involved in this fraction. Ash content depends on the raw material and is usually treated as inert, and its possible catalytic effect on biomass degradation is neglected.

The devolatilization of the biomass is thus considered a straightforward combination of the pyrolysis of three reference components: cellulose, hemicellulose, and lignins. This three-component mechanism has been widely applied to describe TG

curves of biomass devolatilization.<sup>18–20</sup> A large set of encouraging comparisons with several experimental TG curves of pure reference species and different biomasses at variable heating rates (reported and discussed elsewhere) support this approach.<sup>21</sup> Further activities in the development of more detailed mechanisms, which include cross-interactions as well as the chemistry of extractives, should be addressed in the near future.

The characterization of a biomass is then reduced to the definition of the composition of its reference components. When the biochemical analysis is available, it is possible to derive the proper biomass composition details in terms of humidity, ash, cellulose, hemicellulose, and lignin content. If only elemental analysis in terms of C/H/O content is accessible, then a suitable combination of the reference species can be derived by atomic balances as described by Cuoci et al.<sup>22</sup>

The pyrolysis of reference components, presented in this paper and described in the next paragraphs, consists of a limited number of devolatilization reactions, which are applied to predict not only the rate of weight loss, but also the expected composition of species released in the gas and vapor phases.

(20) Orfao, J. J. M.; Antunes, F. J. A.; Figueiredo, J. L. Pyrolysis kinetics of lignocellulosic materials—3 independent reactions model. *Fuel* **1999**, *78*, 349–58.

(21) Faravelli, T.; Frassoldati, A.; Ranzi, E.; Hugony, F.; Migliavacca, G. Modellazione dettagliata della pirolisi di biomasse: Modelli cinetici di devolatilizzazione. *La Rivista dei Combustibili* **2007**, *61* (5), 249–270.

(22) Cuoci, A. T.; Faravelli, A.; Frassoldati, S.; Granata, G.; Migliavacca, E.; Ranzi, S.; Sommariva, A. General Mathematical Model of Biomass Devolatilization, 30th Meeting of the Italian Section of the Combustion Institute; 2007.

(18) Varhegyi, G.; Antal, M. J.; Jakab, E.; Szabo, P. Kinetic modeling of biomass pyrolysis. *J. Anal. Appl. Pyrol.* **1996**, *42*, 73–87.

(19) Teng, H.; Wei, Y. C. Thermogravimetric studies on the kinetics of rice hull pyrolysis and the influence of water treatment. *Ind. Eng. Chem. Res.* **1998**, *37*, 3806–11.



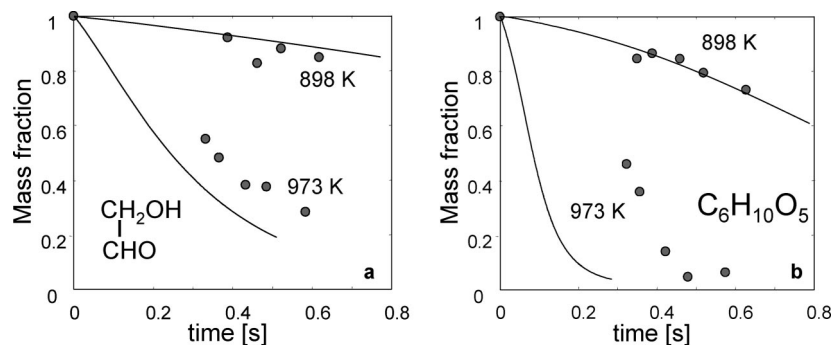


**Figure 6.** Relevant species of devolatilization of cellulose. Decomposition of hydroxyl-acetaldehyde (a) and LVG (b). Comparisons between model predictions (lines) and experimental measurements (points).<sup>17</sup>

**Table 4**

	softwood (wt %)	hardwood (wt %)
cellulose	40.1	49.8
hemicellulose	26.7	33.2
lignins	33.2	17.0

**Table 5. Predicted Volatile Species from Hardwood and Softwood Biomass Degradation at 60 K/min**

	softwood (wt %)	hardwood (wt %)
H <sub>2</sub>	0.65	0.72
H <sub>2</sub> O	4.45	3.83
CO	4.22	3.41
CO <sub>2</sub>	7.13	8.58
CH <sub>4</sub>	0.25	0.17
CH <sub>2</sub> O	2.22	3.06
CH <sub>3</sub> OH	4.75	3.64
C <sub>2</sub> H <sub>4</sub>	0.49	0.30
C <sub>2</sub> H <sub>5</sub> OH	0.57	0.86
acetaldehyde	0.39	0.34
glyoxal	0.19	0.28
HAA	0.74	1.10
propanal	3.23	1.77
CH <sub>3</sub> COCH <sub>3</sub>	0.36	0.22
C <sub>3</sub> H <sub>4</sub> O <sub>2</sub>	0.17	0.11
HMFU	0.41	0.61
phenol	0.34	0.21
LVG	24.62	36.90
xylofuranose	2.10	3.15
methoxy-guaiacol	0.74	0.46
C <sub>11</sub> phenol species	17.37	10.75
solid residue	24.60	19.51

The proposed kinetic schemes adopt both grouping of similar components and lumping of reactions as a compromise capable of satisfactorily describing a variety of biomasses. However, a flexibility in the level of simplification is maintained for the aim of a better comparisons between model predictions and experimental measurements.

Process simulations show that the reference component hemicellulose decomposes at lower temperatures, cellulose requires higher temperatures, whereas lignin decomposes slowly over a broad range of temperatures.

A relevant feature of the proposed kinetic models, when compared with the majority of the available ones, is the effort and the challenge to define a lumped stoichiometry of the devolatilization reactions and to characterize the gas and the tar fractions using a limited number of components.

**2.1. Pyrolysis of Cellulose.** Figure 1 schematically shows the pyrolysis of cellulose, a regular polymer of glucosidic monomers (C<sub>6</sub>H<sub>10</sub>O<sub>5</sub>)<sub>n</sub>. This mechanism refers to the initial formation of an intermediate active cellulose (CELLA), as suggested by several authors.<sup>23–27</sup>

Levoglucosan (LVG: 1,2-anhydro- $\alpha$ -D-glucopyranose, C<sub>6</sub>H<sub>10</sub>O<sub>5</sub>) is then formed from cellulose degradation through a

chain-end depolymerization reaction.  $\beta$ -scission reactions inside the polymer chain and successive molecular and radical reactions are responsible for the formation of hydroxy-acetaldehyde (HAA: C<sub>2</sub>H<sub>4</sub>O<sub>2</sub>), glyoxal (C<sub>2</sub>H<sub>2</sub>O<sub>2</sub>), CH<sub>3</sub>OH, CH<sub>2</sub>O, CO, and CO<sub>2</sub>. A significant amount of 5-hydroxymethyl-furfural (HMFU) together with acetaldehyde and propanal are also observed. The formation of these products directly from cellulose degradation (and not from LVG) has been demonstrated by Banyasz et al.<sup>25,26</sup> The lumped species HAA is supposed to also contain the isomer component acetic acid. The char residue is usually below 5%, depending on operating conditions and uncertainty on experimental devices as suggested by Suuberg et al.<sup>28</sup>

Levoglucosan is always a major product and mainly prevails at low temperatures; its successive vaporization, at about 260 °C, might be a rate-limiting step. The higher the temperature is, the greater the importance and the formation of the remaining degradation products. Among them it is worth mentioning HAA, which becomes significant at temperatures higher than 450–500 °C. Mass transport resistances in the solid matrix and in the melt phase also increase the relative importance of the successive decomposition reactions and char formation. The multistep kinetic scheme of cellulose pyrolysis, with a lumped description of the released species, is reported in Table 1. The rate parameters of the reactions are mainly derived from TG experiments at different heating rates, as well as obtained from a semidetailed kinetic scheme.<sup>29</sup>

How gas and tar components are released by cellulose is discussed in detail in the work of Piskorz et al.<sup>24</sup> From those observations, the equivalent mechanism and the reference “lumped” components have been derived. A sample of comparisons between experimental measurements and model predictions is reported in Figure 2.

Figure 2a reports the comparison between predictions and experiments of cellulose pyrolysis versus heating rate. Figure 2b shows a comparison of predicted and experimental yields

(23) Bradburry, A. G. V.; Sakai, Y.; Shafizadeh, F. *J. Appl. Polym. Sci.* **1979**, *23*, 3271.

(24) Piskorz, J.; Radlein, D.; Scott, D. S. On the mechanism of the rapid pyrolysis of cellulose. *J. Anal. Appl. Pyrol.* **1986**, *9*, 121–37.

(25) Banyasz, J. L.; Li, S.; Lyons-Hart, J. L.; Shaker, K. H. Cellulose pyrolysis: The kinetics of hydroxyacetaldehyde evolution. *J. Anal. Appl. Pyrol.* **2001**, *57* (2), 223–248.

(26) Banyasz, J. L.; Li, S.; Lyons-Hart, J. L.; Shafer, K. H. Gas evolution and the mechanism of cellulose pyrolysis. *Fuel* **2001**, *80* (12), 1757–1763.

(27) Luo, Z.; Wang, S.; Liao, Y.; Cen, K. Mechanism study of cellulose rapid pyrolysis. *Ind. Eng. Chem. Res.* **2004**, *43* (18), 5605–5610.

(28) Suuberg, E. M.; Milosavljevic, I.; Vahur, O. *Proc. Comb. Institute* **1996**, *26*, 1515.

(29) Marongiu, A. Ph.D. Thesis, Politecnico di Milano, Italy, 2005.

(30) Milosavljevic, I.; Suuberg, E. M. *Ind. Eng. Chem. Res.* **34** (4), 1081–1091.

(31) Radlein, D.; Piskorz, J.; Scott, D. S. *J. Anal. Appl. Pyrol.* **1991**, *19*, 41–63.

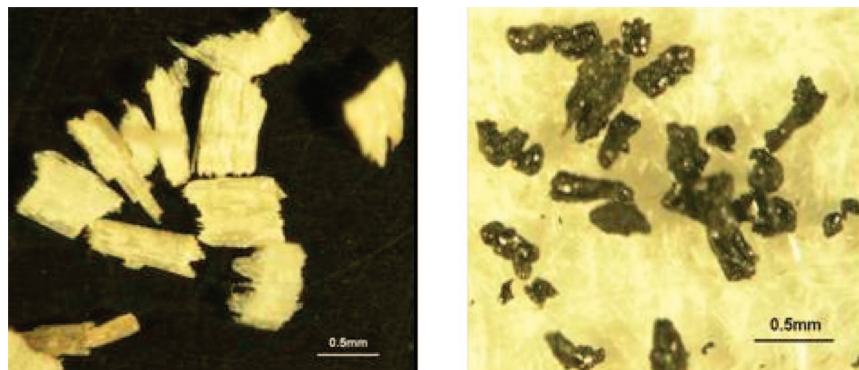


Figure 7. Morphological changes of 0.4 mm particles treated at 1073 K in the drop tube.<sup>6</sup>

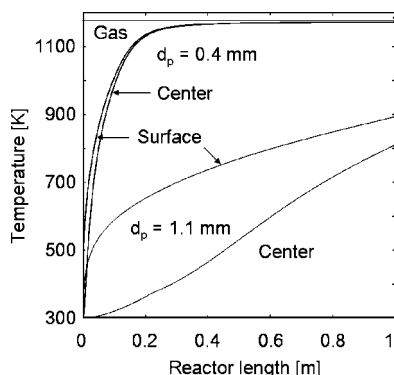


Figure 8. Surface and inner temperature profiles for the different particles.

of LVG and HAA at different temperatures. It is relevant to observe that the lumped component LVG stands also for cellobiosan, whereas acetic acid is included in HAA.

**2.2. Pyrolysis of Hemicellulose and Lignin.** Similarly to cellulose, the hemicellulose and lignin pyrolysis processes were investigated. The same approach and methodologies adopted for cellulose were also applied for these components.

In the scope of this paper, hemicellulose chemical structure is approximated as a xylose polymer  $(C_5H_8O_4)_n$ . Real hemicellulose is a matrix of different polysaccharides and contains mannuronic and galacturonic acids. Typical monomers are glucose, xylose, mannose, galactose, rhamnose, and arabinose. Hemicellulose is easily devolatilized or hydrolyzed by dilute acid or base. Compared with cellulose that is mostly crystalline, strong, and resistant to hydrolysis, hemicellulose has a more random and amorphous structure.

The major features of the kinetic model, including a detailed comparison with experimental measurements, are reported by Faravelli et al.<sup>21</sup> The brief description reported in the following refers to that reference.

Decomposition of hemicellulose (HCE) starts at a temperature lower than that at which cellulose does and forms a 20–25% residue that slowly releases  $H_2$  and CO at higher temperatures. To correctly predict this behavior, the kinetic model reported in Table 2 refers to the intermediate species HCE1 and HCE2 that are involved in successive decomposition reactions with different activation energies and different charring propensity.

Xylose monomer, obtained via HCE1 only, is here considered as a relevant component of the tar fraction. To better describe the devolatilization rate and the widespread gas release, some intermediate components form lumped pseudospecies ( $G\{CO_2\}$ ,  $G\{CO\}$  and  $G\{COH_2\}$ ) trapped in the condensed phase and/or in the solid matrix, which are prone to be released as gas components, with suitable kinetic rates. For instance, the

following first-order kinetic parameters are assumed for loose and tight  $CO_2$  and CO release:

$$G\{CO_2\} \rightarrow CO_2 \quad k = 1 \times 10^5 \exp(-24000/RT) [s^{-1}] \quad (1)$$

$$G\{CO\} \rightarrow CO \quad k = 1 \times 10^{13} \exp(-50000/RT) [s^{-1}] \quad (2)$$

$$G\{COH_2\} \rightarrow CO + H_2 \quad k = 5 \times 10^{11} \exp(-65000/RT) [s^{-1}] \quad (3)$$

Figure 3a shows a sample of comparisons between the experimental measurements of Williams and Besler<sup>32</sup> and model predictions.

Lignins are complex racemic polymers mainly derived from hydroxycinnamyl alcohol monomers with different degree of methoxylation. The complex chemical structure of lignins requires the adoption of different reference components: this means that the lignins are approximated, case to case, by a mixture of reference components. They are identified by LIG-C, LIG-O, and LIG-H, which recall their characteristic of being richer in carbon, oxygen, and hydrogen, respectively. All the reference components are based on the typical  $\beta$ -O-4 skeleton and are shown in Scheme 1.

The reference components decompose, release gases, and form intermediate components that are involved in substitutive additions and cross-linking reactions with a progressive charification of the solid residue. Phenol and phenoxy species become typical products of lignin decomposition. The major features of lignins devolatilization, including a detailed comparison with experimental measurements, are also reported in Faravelli et al.<sup>21</sup> Table 3 summarizes the kinetic model.  $C_9H_{10}O_2$  (paracoumaryl alcohol) and  $C_{11}H_{12}O_4$  stand for the whole class of substituted phenol components, with different methoxyl content.<sup>33</sup> Figure 3b shows two comparisons with TG experimental measurements by Jakab et al.<sup>34</sup> relating to two lignins derived from *Liriodendron tulipifera* and from *Arachis hypogaea*.

### 3. Thermal Degradation of Biomasses

Although extensive and detailed comparisons between model prediction and experimental TG curves are reported in Faravelli et al.,<sup>21</sup> only a couple of examples are here discussed. These experimental data refer to two typical biomasses: softwood bark and hardwood rich in fibers. The C/H/O weight content of these

(32) Williams, P. T.; Besler, S. *Renewable Energy* **1996**, 7 (3), 233–250.

(33) Demirbas, A. The influence of the temperature on the yields of compounds existing in bio-oils obtained from biomass samples via pyrolysis. *Fuel Process. Technol.* **2007**, 88, 591–597.

(34) Jakab, E.; Faix, O.; Till, F.; Székely, T. J. *Anal. Appl. Pyrol.* **1995**, 35, 167–179.



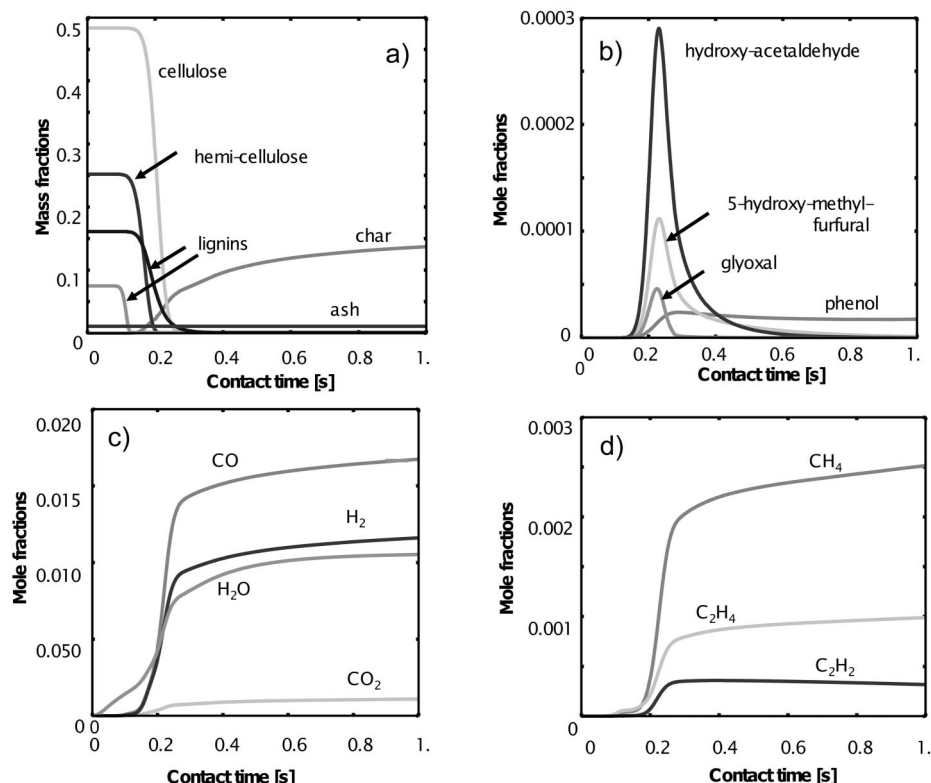


**Figure 9.** Model predictions for the devolatilization of biomass at 1073 K: (a) biomass reference species, ash, and char; (b) relevant intermediate and tar components; (c) major gas components; (d) methane and C<sub>2</sub> components.

biomasses are 53.2/6.0/40.4 and 49.9/6.0/43.8, respectively.<sup>35</sup> The compositions of the reference species are described in Table 4.

A short discussion on the biochemical characterization of the biomasses using only the elemental analysis (H/C/O) is reported in the Supporting Information. Figure 4 shows the thermal degradation of these biomasses at two different heating rates. The model predictions of the hardwood sample are satisfactory, whereas the softwood biomass pyrolysis is slightly slower than its prediction. The behavior in this situation seems to be of unsystematic nature. A possible hypothesis comes from the observations of Williams and Besler;<sup>32</sup> they show that even a low concentration of ashes and impurities can either catalyze or inhibit biomass devolatilization.

Table 5 reports the predicted volatile species from hardwood and softwood biomass degradation at 60 K/min, together with the solid residue. Because of the moderate temperature, still there is ~20% of oxygen and ~2.5% of hydrogen in the predicted weight composition of the solid residue. The larger residue observed in the softwood sample is simply the consequence of the greater amount of carbon and lignin content. Levoglucosane is the most abundant volatile species, and this is due to the large amount of cellulose in both the samples and to the relatively low degradation temperature (see Figure 2b). Phenol and phenolic species are represented by only a couple of lumped species, and they are more abundant from softwood biomass pyrolysis.

Direct comparisons of these predictions with experimental data are only partial and difficult, not only for the limited availability of reliable quantitative measurements, but mainly for the presence and the effect of the secondary gas phase reactions of the released products. The high temperatures of the pyrolysis process and the moderate stability of the volatile species make difficult the direct comparisons of predicted values

and experimental measurements. In fact, large amounts of permanent gases, including methane and C<sub>2</sub> species (C<sub>2</sub>H<sub>4</sub> and C<sub>2</sub>H<sub>2</sub>), are more likely the result of secondary reactions in the gas phase than of the direct release from the biomass. The product distributions reported in Table 5 are then the “a priori” predictions of the proposed model and are only partially the result of preliminary comparison with experimental information. Accurate and reliable comparisons with experimental measurements can be obtained only after the proper understanding of the role of secondary gas phase reactions.

#### 4. Secondary Reactions in the Gas Phase. Gas Phase Kinetics of Released Species

The volatile components may undergo successive decomposition or combustion reactions in the surrounding gas phase. The description of the involved reactions was obtained by enlarging an existing kinetic scheme for the pyrolysis and oxidation reaction of hydrocarbon species.<sup>36</sup> Due to its modular and mechanistic nature, it is sufficient to include the primary propagation reactions of the new species released from the biomasses. Typically, they are initiation and H abstraction reactions of these species and their successive decomposition reactions until the formation of intermediate products already present in the existing kinetic scheme. The thermodynamic properties of the involved species as well as the complete set of primary propagation reactions are reported in the Supporting Information to this paper. These data are also available at the Web site <http://www.chem.polimi.it/CRECKModeling/>.

As an example of the reactivity of released species, Figure 5a shows a comparison of model predictions and the experimental decomposition of 5-hydroxymethyl-furfural, a typical primary product from biomass devolatilization.

These experimental data refer to a quasi-isothermal tubular quartz reactor, where product decompositions of over 50% are

(35) García-Pérez, M.; Chaala, A.; Pakdel, H.; Kretschmer, D.; Roy, C. *J. Anal. Appl. Pyrol.* **2007**, *78*, 104–116.

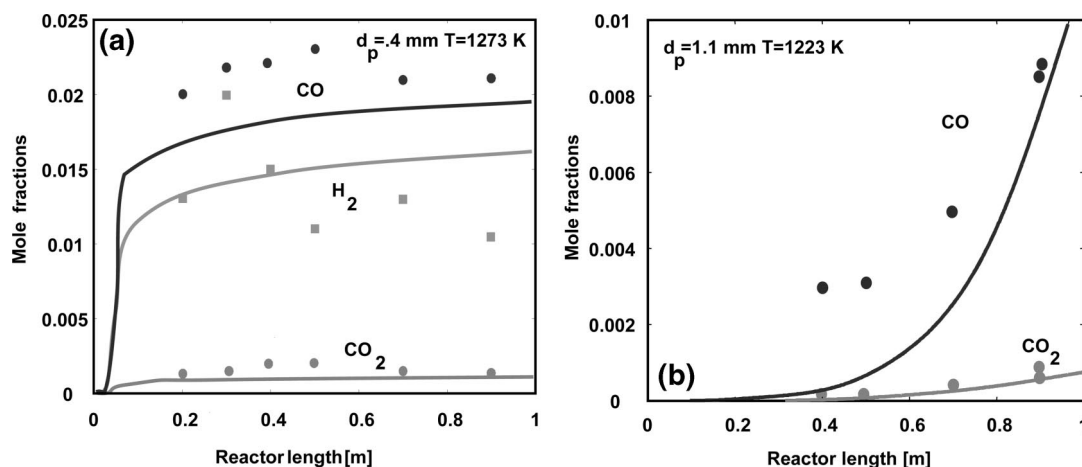


**Figure 10.** Effect of particle diameter. Comparisons between experimental data (points) and model predictions (lines) for 0.4 mm and 1.1 mm particles, at high temperature (1223–1273 K).

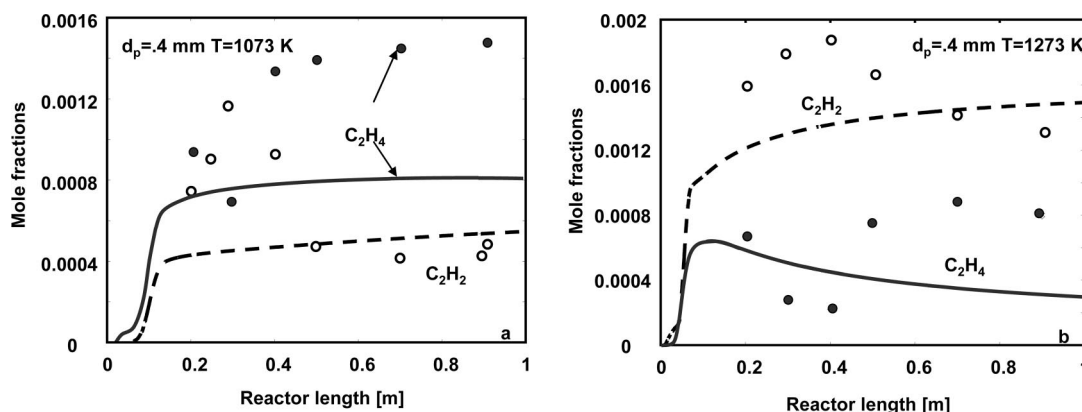
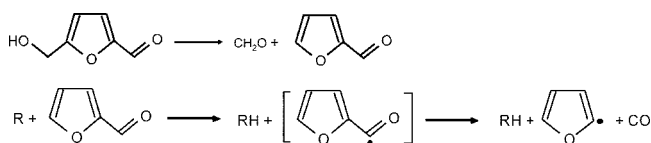


**Figure 11.** Temperature effect on minor species. Comparisons between experimental data (points) and model predictions (lines) at 1073 and 1273 K for 0.4 mm particles.

obtained in less than 1 s at 898 and 973 K.<sup>17</sup> Figure 5b shows the predicted mass fractions of important intermediate products: furfural, CO, and benzene.

Although furfural is a primary intermediate, benzene is mainly the result of the successive recombination and condensation reactions of propargyl radicals.



Two primary steps of the decomposition mechanism of 5-hydroxymethyl-furfural are a molecular and a radical reaction path. Following these reaction paths, 5-hydroxymethyl-furfural forms furfural which in turn, via H abstraction reactions and CO formation, explains the successive formation of furan. The kinetics of furan pyrolysis have been investigated experimentally by Organ and Mackie<sup>37</sup> and theoretically by ab initio quantum chemical techniques.<sup>38</sup> Principal products are carbon monoxide, C<sub>3</sub>H<sub>4</sub> (propyne and allene), and acetylene, together with ketene. Furan consumption is ruled by 1,2-H transfers that result in the

formation of cyclic carbene intermediates whose successive decomposition forms either CO and propyne or C<sub>2</sub>H<sub>2</sub> and ketene, as major and minor channels, respectively.

The experimental work of Shin et al.<sup>17</sup> gives also information on the gas phase conversion of hydroxyl-acetaldehyde and LVG in the same conditions of the quasi-isothermal tubular quartz reactor. Figure 6 shows the comparisons between model predictions and the experimental decompositions. The model seems to overestimate the reactivity at higher temperature, but the overall trends are well reproduced.

Further refinements of the proposed models should be addressed and easily obtained, when new experimental data in different operating conditions will be available. As already mentioned, the proposed approach and model details can be modified and/or extended with the aim of a better characterization of final products and pollutant emissions from biomass devolatilization.

## 5. Application Example: Biomass Devolatilization in a Drop Tube Reactor

Biomass devolatilization in a drop tube reactor is here analyzed in Figure 7 as a first application example of the proposed approach.<sup>6</sup>

The biomass is a mixture of softwoods (Scots pine and spruce) particles with an average diameter of ~0.4 mm. The reactor consists of an alumina tube heated in an electric oven. A preheated N<sub>2</sub> stream (800–1000 °C) and solid particles are separately injected at the top of the reactor. The gas flow is highly laminar (*R<sub>e</sub>* < 200) and the reactor is isothermal in the

(36) Ranzi, E.; Dente, M.; Goldaniga, A.; Bozzano, G.; Faravelli, T. *Prog. Energy Combust. Sci.* **2001**, 27, 99–139.

(37) Organ, P. P.; Mackie, J. C. Kinetics of pyrolysis of furan. *J. Chem. Soc., Faraday Trans.* **1991**, 87 (6), 815–823.

(38) Sendt, K.; Bacskey, G. B.; Mackie, J. C. Pyrolysis of furan: Ab initio quantum chemical and kinetic modeling studies. *J. Phys. Chem. A* **2000**, 104 (9), 1861–1875.

zone within 0.30 and 0.95 m from the solid injection. The contact time of the solid is  $\sim 1$  s.

Model predictions allow the simulation of the different facets of the heating and devolatilization process. Figure 8 shows the surface and inner temperature profiles for the different particles. The small biomass particles quickly reach the gas temperature and are nearly isothermal. Char formation and devolatilization processes are largely completed and qualitatively mimic the experimental transformation shown in Figure 7. On the contrary, large particles show large internal temperature gradients and leave the reactor at moderate temperature without a complete devolatilization.

The release of the major tar components and their successive decomposition to form the final gas products is estimated with great detail and allow comparison with the experimental measurements. Figure 9 shows a detailed description of these processes, including CHAR formation from small particles at 1073 K.

The temperature does not significantly affect CO and H<sub>2</sub> formation because the devolatilization process is practically completed even at 1073 K. Cellulose, hemicellulose, and lignin species undergo decomposition after  $\sim 0.15$  s (at temperatures higher than 500 °C) and then move through different intermediates up to the final formation of the char residue. Figure 9b emphasizes the role of secondary gas phase reactions. Hydroxyacetaldehyde, hydroxymethylfurfural, and glyoxal are completely converted inside the reactor, whereas the less reactive phenol (and phenolic components) are also present in the reactor effluent.

Char is assumed here to be a pure carbon residue. At moderate temperatures and severity, the hydrogen and oxygen content in the solid residue at the reactor outlet is due to unconverted intermediates. The predicted char yield is  $\sim 14$  wt % of the initial dry biomass, which agrees with the experimental measurements. The initial composition of the biomass (C<sub>6</sub>H<sub>8.8</sub>O<sub>3.9</sub>) becomes C<sub>6</sub>H<sub>2.9</sub>O<sub>1.1</sub> at 1073 K and C<sub>6</sub>H<sub>1.4</sub>O<sub>0.5</sub> at 1273 K, at the reactor outlet. These results are in agreement with the experimental measurements indicating a composition of C<sub>6</sub>H<sub>2.7</sub>O<sub>0.8</sub> and C<sub>6</sub>H<sub>1.5</sub>O<sub>0.4</sub>, respectively.

About 90% of initial oxygen in biomass is converted into CO and H<sub>2</sub>O. H<sub>2</sub>, CO, and H<sub>2</sub>O are the major gas components; CO<sub>2</sub> and CH<sub>4</sub> are 1 order of magnitude less, and C<sub>2</sub>H<sub>4</sub> and C<sub>2</sub>H<sub>2</sub> are mostly secondary products, present at ppm levels in the entrainer gases. Similar amounts of benzene and heavier aromatic hydrocarbons are also predicted.

Figures 10 shows the predicted evolution of the main reactants and products, including the final char and 11a compare experimental data and predicted results. CO is the major gas species in both model and experiments, followed by H<sub>2</sub> and H<sub>2</sub>O. There is also a good agreement on CO<sub>2</sub>, which is present only in small amounts. Tar species decompose in the gas phase and significantly contribute to the release of major gases and also to the formation of methane, acetylene, ethylene, and heavier hydrocarbons. Figure 10 clearly shows the effect of particle size; the largest particles are only "roasted" or "toasted", without completing the devolatilization process.

Acetylene and ethylene predictions agree with the experimental measurements (Figure 11). In fact, C<sub>2</sub>H<sub>2</sub> is more abundant than C<sub>2</sub>H<sub>4</sub> at high temperatures, whereas the reverse behavior is predicted and measured at 1073 K. The model

underestimates methane formation of about 30–40%. Further kinetic analysis and further experimental activity are required to better understand the formation of methane and methyl radicals from biomass and intermediate tar components.

The comparisons of Figure 10 and 11 indicate the ability of the model to predict not only the amount and composition of the solid residue, but also the ability to characterize minor components in the gas phase. These results demonstrate the importance of the successive gas phase reactions.

As far as the kinetics of gasification and combustion of char residue is concerned, it is assumed that only the final char residue is reactive and the usual kinetic laws of pure carbon oxidation are applied.<sup>39</sup> Note that gasification reactions are too slow to occur under the conditions of the present example.

## 6. Conclusions

To predict gas composition from industrial biomass gasifiers, it is crucial to describe and properly combine the four different features of this complex process:

- Biomass characterization
- Solid fuel devolatilization
- Secondary reactions in the gas phase.
- Char gasification

Biomass characterization is considered a straightforward combination of three reference components: cellulose, hemicellulose, and lignins.

Kinetic models of the different steps of solid fuel volatilization and secondary gas phase reactions were developed and validated through comparison with experimental data. Despite their simple expressions, these models allow the characterization of the degradation steps, their characteristic times, and the prediction of product distributions. These aspects make the proposed mechanisms a useful tool in the design and optimization of industrial gasifiers, where the presence of tars needs to be either enhanced or lowered. The focus on product and byproduct formation is a further advantage when considering pollutant emission from such devices.

This work has faced the above subjects with the ambitious aim of adding further steps to a difficult path. The complexity of the proper characterization of biomass structures and the large number of intermediates force the use of drastic simplifications. It is clear that this pyrolysis model is only a first and preliminary step and that further efforts and tailored experiments are required for improving the reliability of the overall kinetic model.

**Acknowledgment.** We gratefully acknowledge the financial support of the MIUR-FIRB projects and Progetto ex DM593/2000 (prot. No. 13569 of 28/12/2001). We also acknowledge ENEA for its financial support and CEA (Grenoble, France) for providing the experimental data of Figure 7, 10, and 11.

**Supporting Information Available:** Additional materials mentioned within the text are separately provided. This material is available free of charge via the Internet at <http://pubs.acs.org>.

EF800551T

(39) Branca, C.; Di Blasi, C.; Horacek, H. *Ind. Eng. Chem. Res.* **2002**, *41* (9), 2107–2114.